ETH
Eidgenössische Technische Hochschule Zürich
Swiss Federal Institute of Technology Zurich

Merging Properties of a Cellular Automaton for Blocking Queen Games

Bachelor Thesis

A. Peter

September 22, 2022

Advisors: Dr. M. Cook, Prof. Dr. A. Steger, E. Palmiere
Department of Computer Science, ETH Zürich

Acknowledgements

First and foremost, I would like to express my gratitude to Dr. Matthew Cook and his research group for enabling me to work on this topic. His expertise in the topic and guidance throughout this process has had a great influence on the present work and provided the foundation for it. I would also like to thank Ethan Palmiere for supervising the thesis and providing professional feedback. I wish to extend my special thanks to Rupert Hitsch and my family for reading the thesis and giving suggestions as well as to Benjamin Unger for going through the proofs. Lastly, I wish to show my appreciation to Prof. Dr. Angelika Steger and her research group for enabling me to complete this thesis at the Department of Computer Science and for the continuing collaboration between the two groups.

Abstract

This thesis provides an in-depth analysis of a substructure, called the *warp*, of a cellular automaton for blocking queen games proposed by Cook, Larsson and Neary in 2016 [5]. We show that a simple toy model can be used to examine threads of winning positions in the warp and present several findings relating to the number sequences they produce. The game of interest, *k-blocking Wythoff Nim*, may be summarized as a game where the moves correspond to moving a queen in chess, but only towards $(0, 0)$ and with the restriction that an opposite player may block up to $k - 1$ positions temporarily. As soon as a player reaches the origin, the game ends and the last player to move wins. The game gives rise to highly complex structures which are mostly sensitive to the parameter k. However, the threads of winning positions in the warp seem to have consistent thicknesses which add up to Fibonacci numbers. The final toy model we propose exhibits the same merging property as the cellular automaton and gives rise to a class of toy models based on the infinite Fibonacci word.

Contents

Chapter 1

Introduction

The original Nim game was proposed by C. L. Bouton in 1901 [4]. In the simplest form, it is played with two players and three initial piles containing any number of tokens. In each turn, a player may remove an arbitrary number of tokens from any pile, taking at least one token. The player who takes the last token(s) wins. Remarkably, by remembering a formula for the set of winning positions, the skilful player can secure a 100% chance of winning when the right number of tokens are set out initially.

To make things more interesting, W. A. Wythoff proposed a slight modification of this game in 1907 [20]. Contrastingly, Wythoff Nim is played only with two piles of tokens and with two players. In each move, a player may either remove the same number of tokens from both piles or some tokens from one pile, taking at least one token. Again, the player who removes the last token(s) wins. A set of winning positions closely related to multiples of the golden ratio has been found by Wythoff [20].

K-blocking Wythoff Nim as proposed in 2010 [11], the game of interest in this thesis, performs a slight modification on Wythoff Nim. Namely, a blocking maneuver whereby a player can declare at most $k-1 \geq 0$ positions forbidden for the next player is added. Similar to the other two games, we are interested in finding winning positions, so-called *P-positions*, which will be defined in more detail later. Since these positions could be expressed by number sequences for Nim and Wythoff Nim, the question of whether a similar approach can be applied to blocking Wythoff Nim arises. Unfortunately, the game of blocking Wythoff Nim for general k has proven to be much more complicated. Only the asymptotic 'behaviour' in terms of sets of aggregation points for P positions for $20 \geq k > 3$ was conjectured with the aid of computer simulations [11].

This motivated the work of Cook, Larsson and Neary in [5]. In the cited paper, the authors specified a cellular automaton which generates the P-positions

for any number k of blocking positions.[1] The cellular automaton exhibits many interesting, unexplored properties and thus gives rise to a plethora of research questions. Specifically, there is a substructure, called the *warp*, where some regularity in a thread-merging process of P-positions can be witnessed. We will later define what a thread is and how threads merge, but it can be considered to be a group of P-positions roughly aligned along a line until then. Moreover, it has been empirically observed that the thread thicknesses always merge to Fibonacci numbers. This thesis more closely examines this phenomenon and attempts to take an isolated view by creating a toy model exhibiting similar properties. Therefore, we examine the following research question (posed in [5]) to gain a more refined understanding of the cellular automaton:

> *Why is it that the threads of the warp merge in such a way that their thickness is always a Fibonacci number?*

[1] In the next chapter, we will describe cellular automata in more detail. As of now, it suffices to think of it as some model which can perform certain computations.

Chapter 2

Background

In this chapter, we introduce and explain the theoretical background on top of which this thesis lies. That is, we will take a brief look into the essentials of combinatorial game theory and define some terminology. We define the game of interest, k-blocking Wythoff Nim, as well as cellular automata as a general computational tool. Finally, the mathematical background necessary to analyze and devise the toy models is established.

2.1 Combinatorial Game Theory

Combinatorial game theory studies combinatorial games, e.g. all variations of Nim. We hereby recapitulate some essential definitions and terminology which will be used later [2, 13].

Definition 2.1 (Combinatorial Game) *In a combinatorial game, two players take turns making moves. Both players have complete information about the game and there is no chance.*

In contrast to other games, no element of chance (e.g. the shuffling of cards) and hidden information (e.g. cards in the hands of a player) are a part of combinatorial games. In *standard play*, which we will consider for our purposes, the player who runs out of moves first loses.

The game of Nim can be studied very well mathematically because the same strategy can be applied to both players interchangeably, that is, the game is *impartial*.

Definition 2.2 (Impartiality) *In an impartial game, each player has exactly the same moves available from each position. For example, chess is not impartial since one player can only move black pieces whereas the other player can only move white ones.*

Finally, we define sets of positions based on whether moving to such a position is a winning or losing move.

Definition 2.3 (N-position) *A position is an N-position if the player who is next to move (*N-player*) has a winning strategy.*

Definition 2.4 (P-position) *A position is a P-position (also known as* palace position *or* safe combination*) if the player whose turn has just ended (*P-player*, as in the previous player) has a winning strategy.*

At the beginning of the game, it is the *next* player's turn to move. This means that at any point in the game, one would want to play first if the game is at an N-position and second if the game is at a P-position. We shall see later that it is customary to define a game's winning strategy by its P-positions.

2.1.1 K-Blocking Wythoff Nim

Following, we look at the combinatorial game of interest in this thesis, k-blocking Wythoff Nim. As we have seen briefly in the introduction, the game poses a slight modification of Wythoff Nim. We introduce its definition here to recapitulate what was stated above and formalise the game. [11]

Definition 2.5 *Let $k \in \mathbb{N}$. In* k-blocking Wythoff Nim*, denoted by W^k, there are two players and two piles of tokens. A move consists of removing an arbitrary number of tokens greater than zero from a single pile, or the same number of tokens from both piles. Before the next player moves, the previous player may choose at most $k-1$ blocking positions to be inaccessible. The blocking positions can be declared anew at every move.*

K-blocking Wythoff Nim can be equivalently regarded as a blocking queen game if we label the two piles as x and y and define a position (x, y) on the chessboard by the number of tokens left on the two piles. Now the possible moves correspond to moving a queen in chess, but only towards the origin and disallowing blocked positions. The $k-1$ blocked positions can be considered occupied by pawns if we define the game such that the queen cannot move to a position occupied by a pawn, however, it can move over pawns to an empty spot. [5]

2.2 Cellular Automata

In the paper on top of which this thesis lies, a *cellular automaton* (*CA*) for k-blocking Wythoff Nim is introduced. Let us now take a brief look at cellular automata.[1] John von Neumann, inspired by the work of Alan Turing on

[1] We will not go into too much detail here, but refer to works like [10] which provide a great introduction to cellular automata and related systems.

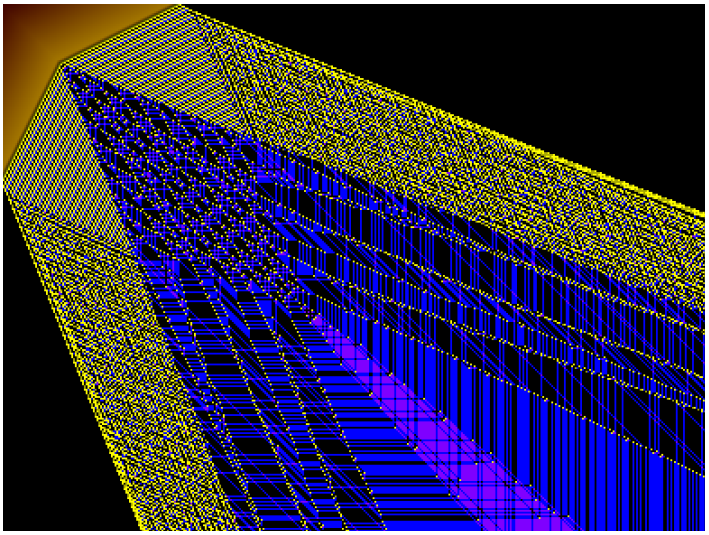

Figure 2.1: A cellular automaton which describes blocking Wythoff Nim for $k = 100$ (Game 100). The coordinates (x, y) of a cell correspond to the number of tokens left on the two piles. Note that the two piles are treated equally in the game and thus the cellular automaton appears symmetrical with respect to a diagonal axis drawn from the origin at the top-left corner.

computability, was the first person to describe *self-reproducing automata* in 1966 [18] as a system which is capable of simple computations. In general, CA are discrete and deterministic mathematical models whose parallel evolution depends on local interaction.

A cellular automaton consists of an n-dimensional grid and cells which have a state. The cells can change state depending on their neighbours' state, where the neighbourhood size can be defined arbitrarily. We usually visualise a CA on a space-time grid where previous states can also be seen. For one-dimensional automata, this would be a two-dimensional grid where one axis symbolises time and the other space. To exemplify, let us examine the cellular automaton for k-blocking Wythoff Nim seen in Figure 2.1. It is one-dimensional and has a two-dimensional space-time grid, where a cell can be considered to be a square on this grid. Further, the state update rule is based on the states of the two parent cells, the state of the central grandparent cell *and* the states of its parents and central grandparent. This makes the cellular automaton a one-dimensional CA of fourth order (since the neighbourhood in consideration goes back *four* generations). For a more detailed description of this CA including its connection to the game, we refer to the work of Cook, Larsson and Neary [5].

2.2.1 Merging Properties of the Cellular Automaton

In this section, we examine the cellular automaton for blocking queen games in more detail and set out the preliminaries for our toy model. That is, we

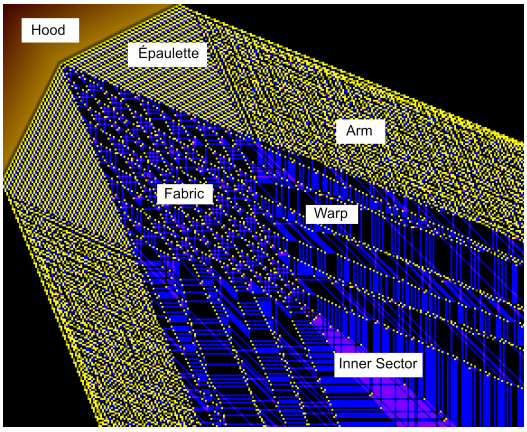

Figure 2.2: A zoomed-in image of Game 100 with the regions of importance for this thesis named.

need to understand the behaviour that it should model. As mentioned in the introduction, we would like to have a model whose behaviour closely mirrors the thread-merging process in the cellular automaton for k-blocking Wythoff Nim proposed in [5]. Figure 2.1 shows the aforementioned cellular automaton for $k = 100$ blocking positions. It is visible that this CA comprises many non-trivial structures, nonetheless, it can be clearly divided into several areas of interest, which can be seen in Figure 2.2.[2] We will from now on restrict ourselves to the study of the *warp*, which refers to the two symmetric areas where we see disconnected, diagonal yellow lines (which we will call *threads*, see Definition 4.1 below). While we do not need to know about the meaning of the colour scheme in detail for now, it should be noted that a yellow position signifies that at most $k - 1$ winning positions are visible (which could all be blocked, cf. Definition 2.5). So the yellow positions mark P-positions as we defined them in Section 2.1, as it is favourable for a player to move to such a position.

Thickness Addition

An important insight of previous empirical studies of the warp are the witnessed thicknesses which were found to be members of the Fibonacci numbers. The *thickness* of a thread in the upper warp is defined as the number of yellow positions (visible as pixels) seen horizontally per thread. Note that since the cellular automaton is symmetric, there are two warps. We will from now on restrict ourselves to the top warp (for the bottom warp, everything would be flipped, so the thickness is measured vertically). In Figure 2.3, the thread thicknesses and the way they merge are depicted. Note

[2] We follow the same terminology as in [5], but do not include all regions as we focus mainly on the threads in the warp and how they emerge from the fabric.

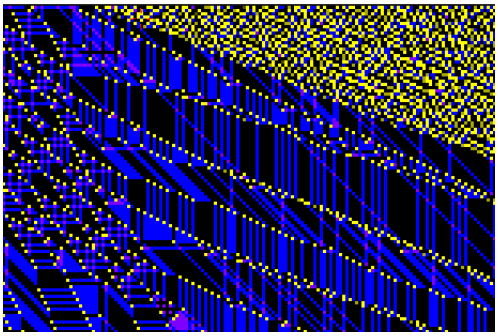

(a) Thread view of Game 100.

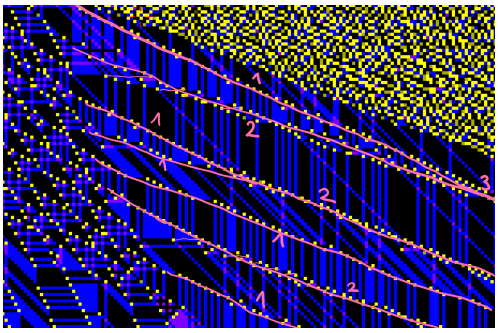

(b) Same as above, with the threads and their thicknesses highlighted in pink.

Figure 2.3: A zoom-in of the warp of the cellular automaton shown in Figure 2.1. We can see the threads as the diagonal yellow lines moving from the top left to the bottom right corner and the thicknesses highlighted in pink (Figure 2.3b).

that when two threads collide, it was observed that their thicknesses add. For example, in Figure 2.3b, we identify a thread of thickness 1 and one of thickness 2 merging to form a bigger thread whose thickness is $2 + 1 = 3$. To explain this observation, we can consider what happens to the number of P-positions visible after a collision of two yellow threads. The number of winning moves seen for every position mirrors how many palaces can be seen moving vertically up, horizontally to the left and diagonally to the top-left corner. Since the number of P-positions before and after the yellow thread remains constant for both incoming threads, this must also hold for the merged thread. This means that the palaces seen horizontally for the two threads add.

2.3 Mathematical Background

2.3.1 Golden Ratio and Number Sequences

In the following, we examine the mathematical definition of the golden ratio, the Fibonacci numbers and Lucas numbers and include a few formulae which

will be used later. We restrict our study to these number sequences as the Fibonacci numbers have been empirically observed in the cellular automaton (as thread thicknesses) and the Lucas numbers are closely related. Further, the Fibonacci and Lucas numbers satisfy the same recursion formula and both can be expressed in terms of the golden ratio. We also introduce Beatty sequences to describe multiples of the golden ratio. They are closely linked to the final toy model and Wythoff Nim.

Golden Ratio

The golden ratio describes a ratio between two numbers and as such it was first studied in geometry, dating back to 1835 when it first appeared in a German textbook. Yet, the ratio was used much earlier in Greek art since it was perceived to be aesthetically pleasing. It was only later discovered that the golden ratio also has close ties to the Fibonacci numbers through its continued fraction and the closed formula of the sequence. [7]

Definition 2.6 (Golden ratio) *Two numbers a and b with $a > b > 0$ are said to be in the golden ratio if $\frac{a+b}{a} = \frac{a}{b} = \varphi$. Henceforth, we will refer to the golden ratio by φ.*

We also include the derivation of a closed form for φ as it already unveils some remarkable properties [7]. If we look at $a = \varphi$ and $b = 1$ for Definition 2.6, we get:

$$\varphi = 1 + \frac{1}{\varphi}.$$

Now we see that

$$\varphi^2 - \varphi - 1 = 0.$$

Solving this quadratic equation, we get two possible values for φ:

$$\frac{1 \pm \sqrt{5}}{2}$$

Since we defined a ratio between positive numbers (cf. Definition 2.6), φ is the positive root. That is,

$$\varphi = \frac{1 + \sqrt{5}}{2} = 1.618033\ldots$$

The negative solution to this equation has similar properties to φ and we will refer to it as $\overline{\varphi}$. Let us now define the complement of the golden ratio:

Definition 2.7 *The complement of φ, denoted by $\overline{\varphi}$, is defined as:*

$$\overline{\varphi} = \frac{1 - \sqrt{5}}{2} = 1 - \varphi = -\frac{1}{\varphi}$$

Fibonacci Numbers

The Fibonacci sequence is one of the most well-studied and famous mathematical number sequences, dating back to Indian scholars in the 1100s (cf. [15]). For the analysis of the cellular automaton for blocking queens, they are of special interest as the thread-merging process happens in Fibonacci numbers. Due to the close ties between φ and Fibonacci numbers, it is natural to introduce their definition next. [15]

Definition 2.8 (Fibonacci numbers) *The Fibonacci numbers are defined by the recursive relation $F_n = F_{n-1} + F_{n-2}$ with $F_0 = 0$ and $F_1 = 1$. From now on, F_n will refer to the nth Fibonacci number.*

Let us use this definition to derive the first few elements of this sequence:

$$0,\ 1,\ 1,\ 2,\ 3,\ 5,\ 8,\ 13,\ \ldots$$

Since recursive formulae are limited and slow to use, we also state the closed formula, using the complement of the golden ratio, $\overline{\varphi}$.

$$F_n = \frac{\varphi^n - \overline{\varphi}^n}{\sqrt{5}} \tag{2.1}$$

This formula allows us to directly compute any member of the sequence and also highlights a relationship to the golden ratio.

The Fibonacci numbers can be generalised to any number sequence following the same recurrence relation.

Definition 2.9 (Generalised Fibonacci sequence) *The generalised Fibonacci sequence is defined by $a, b, a+b, a+2b, 2a+3b, 3a+5b, \ldots$ for some integers a and b.*

The Fibonacci numbers are thus the generalised Fibonacci sequence generated by setting $a = 0$ and $b = 1$.

Lucas Numbers

The Lucas numbers follow exactly the same recurrence relation as the Fibonacci numbers and are therefore also a generalised Fibonacci sequence, but start with a different pair of initial values. The result is remarkably different from the Fibonacci sequence in certain aspects. For example, adding a large Lucas number to the number of blocking positions k seems to result in similar generated patterns in the inner sector (contrary to the addition of a Fibonacci number).

Definition 2.10 (Lucas numbers) *The Lucas numbers are defined by the recurrence equation $L_n = L_{n-1} + L_{n-2}$ with $L_0 = 2$ and $L_1 = 1$. As of now, we will consider L_n to be the nth Lucas number.*

There are several conventions for the first value of the Lucas numbers (either 2 or 1). Following Definition 2.10, we will consider the Lucas numbers starting at 2 (as in [17]) but start indexing at 0 to remain consistent with other sources. Again, let us derive the first few elements of the sequence:

$$2,\ 1,\ 3,\ 4,\ 7,\ 11,\ 18,\ 29,\ \ldots$$

Finally, we write down the closed form of the Lucas numbers which relies on the golden ratio and bears some similarity to the one for Fibonacci numbers.

$$L_n = \varphi^n + \overline{\varphi}^n \tag{2.2}$$

There are several formulae relating the Lucas numbers and the Fibonacci numbers. Here we list two which we will later make use of [17].

$$L_n = F_{n-1} + F_{n+1} \tag{2.3}$$

$$5F_n + L_n = 2L_{n+1} \tag{2.4}$$

Beatty Sequences

The Beatty sequence, named after S. Beatty, was first mentioned in a mathematical problem presented in 1926 [3]. This problem caught the attention of the mathematical community globally and led to various analyses [14].

Definition 2.11 (Beatty sequence) *A Beatty sequence is given by the integer parts of multiples of an irrational number θ: $\lfloor\theta\rfloor$, $\lfloor 2\theta\rfloor$, $\lfloor 3\theta\rfloor \ldots$, where $\lfloor x\rfloor$ is the floor function.*

The problem posed by Beatty was to prove the following [8]:

If α and β are positive irrational numbers such that

$$\frac{1}{\alpha} + \frac{1}{\beta} = 1, \tag{2.5}$$

then all positive integers are contained exactly once by the sequences $\lfloor\alpha\rfloor, \lfloor 2\alpha\rfloor$, $\ldots$ and $\lfloor\beta\rfloor, \lfloor 2\beta\rfloor, \ldots$ The problem has been proven and these two sequences are often referred to as *complementary Beatty sequences*.

Example 2.12 *The Beatty sequences given by $\alpha = \sqrt{2}$ and $\beta = 2 + \sqrt{2}$ are complementary:*

$$\frac{1}{2\sqrt{2}} + \frac{1}{\sqrt{2}} = \frac{\sqrt{2} + 2 + \sqrt{2}}{\sqrt{2}(2+\sqrt{2})} = \frac{2\sqrt{2}+2}{2\sqrt{2}+2} = 1.$$

In subsequent sections, we will also stumble upon the Beatty sequence generated by $\alpha = \varphi$ and its complement $\beta = \varphi^2$ which provide the set of winning positions for Wythoff Nim. Note that they solve Equation 2.5 by the definition of the golden ratio.

2.3.2 Continued Fractions

In this section, we introduce the study of continued fractions. A continued fraction is obtained by iteratively dividing a number into its integer part and the reciprocal of another number. In the case of irrational numbers, such as the golden ratio, this results in an infinite term. For our purposes, it suffices to introduce the *simple* continued fraction, which we will refer to as the *continued fraction* for brevity. We introduce continued fractions here as they will help us with the study of the golden ratio and its relationship to the Fibonacci numbers [12, 19].

Definition 2.13 *A simple continued fraction is an (infinite) expression of the form*

$$a_0 + \cfrac{1}{a_1 + \cfrac{1}{a_2 + \cfrac{1}{a_3 + \cdots}}}$$

where a_k is a possibly infinite sequence of integers such that a_0 is non-negative and the rest of the sequence is positive. The above fraction is often abbreviated as $[a_0; a_1, a_2, \dots]$.

We can approximate any number by truncating the sequence at a_k and computing the resulting expression. This gives us the kth *convergent* $\frac{p_k}{q_k}$ for some positive co-prime integers p_k and q_k. The first three convergents are

$$\frac{a_0}{1}, \frac{a_1 a_0 + 1}{a_1}, \frac{a_2(a_1 a_0 + 1) + a_0}{a_2 a_1 + 1}$$

In general, p_k and q_k are defined by

$$\begin{aligned} p_k &= a_k p_{k-1} + p_{k-2} \\ q_k &= a_k q_{k-1} + q_{k-2} \end{aligned} \tag{2.6}$$

We can define a finite continued fraction directly by the last convergent

$$[a_0, a_1, \dots, a_n] = \frac{p_n}{q_n}$$

Note that by the recursive definition in Equation 2.6, it follows that

$$\frac{p_n}{q_n} = \frac{a_n p_{n-1} + p_{n-2}}{a_n q_{n-1} + q_{n-2}} \tag{2.7}$$

Example 2.14 *The continued fraction of the golden ratio is*

$$1+\cfrac{1}{1+\cfrac{1}{1+\cfrac{1}{1+\cdots}}}$$

We note that its convergents are $\frac{1}{1}, \frac{2}{1}, \frac{3}{2}, \frac{5}{3} \ldots$ *In general, the kth convergent is* $\frac{F_{k+2}}{F_{k+1}}$.

Further, we define the kth complete quotient of the continued fraction $[a_0, a_1, \ldots, a_n]$ of x as

$$a'_k = [a_k, a_{k+1}, \ldots, a_n]$$

and we note that $a'_k \geq a_k$ for all k.

Next, we state a theorem about the convergents of a continued fraction which we will apply in a proof in Section 4.2. A more involved analysis including the proof can be found in [9] and many other resources. To make this thesis self-contained, we also include a slightly adapted version of the proof here. Before we state the proof, we look at two lemmata used in it (the first one was taken from [9]).

Lemma 2.15 *The numbers p_k and q_k satisfy*

$$p_k q_{k-1} - p_{k-1} q_k = (-1)^{k-1}$$

Proof Following Equation 2.6,

$$\begin{aligned} p_k q_{k-1} - p_{k-1} q_k &= (a_k p_{k-1} + p_{k-2})\, q_{k-1} - p_{k-1}\,(a_k q_{k-1} + q_{k-2}) \\ &= -\left(p_{k-1} q_{k-2} - p_{k-2} q_{k-1}\right) \end{aligned}$$

This step can be repeated by replacing k with $k-1, k-2, \ldots, 2$ to obtain

$$\begin{aligned} p_k q_{k-1} - p_{k-1} q_k &= (-1)^{k-1}\,(p_1 q_0 - p_0 q_1) \\ &= (-1)^{k-1} \cdot ((a_1 a_0 + 1) \cdot 1 - a_0 a_1) \\ &= (-1)^{k-1}\,(1) = (-1)^{k-1} \end{aligned}$$

□

Lemma 2.16 *For any x with the continued fraction $[a_0; a_1, \ldots, a_n]$ it holds that* $\frac{a'_{k+1} p_k + p_{k-1}}{a'_{k+1} q_k + q_{k-1}}$ *for any $0 \leq k \leq n$.*

Proof We proceed by induction with the base cases $k = 0$ and $k = 1$. For $k = 0$ we get

$$x = a'_0 = a_0 + \frac{1}{a'_1} = \frac{a'_1 a_0 + 1}{a'_1} = \frac{a'_1 p_0 + 1}{a'_1 q_0 + 0}$$

by using the definitions of p_1 and q_1. We can proceed similarly for $k = 1$ to get

$$\begin{aligned} x &= a_0 + \frac{1}{a'_1} = a_0 + \frac{1}{a_1 + \frac{1}{a'_2}} \\ &= a_0 + \frac{a'_2}{a_1 a'_2 + 1} = \frac{a_0(a_1 a'_2 + 1) + a'_2}{a_1 a'_2 + 1} \\ &= \frac{a_0 a_1 a'_2 + a_0 + a'_2}{a_1 a'_2 + 1} = \frac{a'_2 p_1 + p_0}{a'_2 q_1 + 0} \end{aligned}$$

Let us now assume that $x = \dfrac{a'_k p_{k-1} + p_{k-2}}{a'_k q_{k-1} + q_{k-2}}$. Note that $a'_k = [a_k, a_{k+1}, \ldots, a_n] = a_k + \dfrac{1}{a'_{k+1}}$. Using this, we get

$$x = \frac{\left(a_k + \frac{1}{a'_{k+1}}\right) p_{k-1} + p_{k-2}}{\left(a_k + \frac{1}{a'_{k+1}}\right) q_{k-1} + q_{k-2}}$$

We can now simplify and factor out $\dfrac{1}{a'_{k+1}}$ to get

$$\begin{aligned} x &= \frac{p_{k-1} a_k a'_{k+1} + p_{k-1} + a'_{k+1} p_{k-2}}{q_{k-1} a_k a'_{k+1} + q_{k-1} + a'_{k+1} q_{k-2}} \\ &= \frac{a'_{k+1}(p_{k-1} a_k + p_{k-2}) + p_{k-1}}{a'_{k+1}(q_{k-1} a_k + q_{k-2}) + q_{k-1}} = \frac{a'_{k+1} p_k + p_{k-1}}{a'_{k+1} q_k + q_{k-1}} \end{aligned}$$

□

Now we are well-equipped to prove the following theorem which provides a bound on how good a convergent approximates its continued fraction.

Theorem 2.17 *For any number x with convergents $\dfrac{p_k}{q_k}$,*

$$\left| x - \frac{p_k}{q_k} \right| \leq \frac{1}{q_{k+1} q_k}$$

Proof Recall from Lemma 2.16 that

$$x = \frac{a'_{k+1} p_k + p_{k-1}}{a'_{k+1} q_k + q_{k-1}}$$

Using Lemma 2.15, we can now derive algebraically that

$$\begin{aligned}\left|x - \frac{p_k}{q_k}\right| &= \left|\frac{a'_{k+1}p_k + p_{k-1}}{a'_{k+1}q_k + q_{k-1}} - \frac{p_k}{q_k}\right| = \left|\frac{a'_{k+1}p_kq_k + p_{k-1}q_k - a'_{k+1}q_kp_k - q_{k-1}p_k}{(a'_{k+1}q_k + q_{k-1})q_k}\right| \\ &= \left|-\frac{p_kq_{k-1} - q_kp_{k-1}}{q_k(a'_{k+1}q_k + q_{k-1})}\right| = \left|\frac{(-1)^k}{q_k(a'_{k+1}q_k + q_{k-1})}\right| = \frac{1}{q_k(a'_{k+1}q_k + q_{k-1})} \\ &\leq \frac{1}{q_k(a_{k+1}q_k + q_{k-1})} = \frac{1}{q_{k+1}q_k}\end{aligned}$$

□

Chapter 3

Methodology

Now that we have established the theoretical background for the topic of this thesis, we can set out how to approach the research question. We have already analysed the problem statement in more detail by looking at the cellular automaton, also showing that the thicknesses of threads always add in Section 2.2.1. Next, a generalised toy model can be defined by taking a slightly simplified view of the warp of the CA while keeping the observed properties. This will serve as a foundation for the two toy models which are then derived. The first toy model has the fractional parts of multiples of the golden ratio as its initial slopes, as suggested by previous empirical observations and the second one is based on a number sequence we obtain through the analysis of the first toy model.

Considering that ratios of Fibonacci numbers approximate φ (following the continued fraction of φ in Example 2.14), the first model could be a good approach to generating Fibonacci numbers. A `Java` program which visualises the evolution of threads is written to facilitate the analysis of this model.[1] The complete source code can be found on GitHub [1]. After drawing some empirical observations of this first model, we devise a more mathematical approach to solving the problem. The analysis of Fibonacci numbers and the golden ratio often leads to structures observed in nature, specifically, the way plants grow. Phyllotaxis, which refers to the alignment of leaves, is studied as an aid to improve our understanding of how Fibonacci numbers appear. This and the analysis of the first toy model leads us to the second and final toy model based on a number sequence closely linked to Wythoff's game. After properly analysing this toy model, we relate the findings to the cellular automaton and provide an outlook on future research.

[1] The images showing the evolution of threads in the toy models in Chapter 4 were generated using this code.

Chapter 4

Results

From now on, let us consider a plane in 2D. We define a toy model based on threads (think of them as lines in the plane) and their thicknesses. Further, we abstract away the fact that threads are partly disconnected in the cellular automaton in Figure 2.1 and that thickness in the CA is defined in a slightly more involved manner by connecting pixels via a horizontal line. As such, we will consider the thread thickness to be an inherent property of a thread which is not visible in the graphics and the threads to be connected. Note that the definitions below are therefore adapted to the study of toy models and do not apply the same way in the actual cellular automaton.

Definition 4.1 (Thread) *A thread is a (connected) line which is uniquely defined by its slope $s \in \mathbb{R}$ and its thickness $t \in \mathbb{N}$.*

Two or more threads merge when they collide at the same point in the plane. Upon merging, the respective thicknesses add.

Definition 4.2 (Merging) *When two (or more) threads collide, they combine to form a new thread whose thickness corresponds to the sum of the individual thicknesses. The slope of the new thread amounts to some function of the incoming slopes. We call this process merging and write that the threads merged.*

Finally, we can define a generalised slope system based on threads and merging.

Definition 4.3 (Slope System) *A slope system consists of threads that behave like lines on a plane according to their slopes. The system evolves by the merging of threads and the resulting slopes. It has reached a final state if no two threads can merge anymore.*

The study of toy models here aims to examine various slope systems to come up with an approach that corresponds to the behaviour observed in the cellular automaton. To do this, fitting initial slopes and merging procedures

need to be defined under the primary constraint that threads should always merge such that the resulting thickness corresponds to a Fibonacci number.

4.1 Golden Ratio Slope System

This first approach considers the relationship between the Fibonacci numbers and the golden ratio. Consider the formula for Fibonacci numbers seen in Equation 2.1 or the fact that a Fibonacci multiple of φ approximates another Fibonacci number.[1] This gives us a simple initial state of the system where the threads start with integer multiples of the golden ratio modulo 1 as slopes.

4.1.1 Model Definition

Definition 4.4 *In the initial state, there are n starting threads, where the slope of the kth thread is $s_k = \{k\varphi\}$ and $\{x\}$ denotes the fractional part of x. The kth thickness t_k is 1 for all k. Upon collision of two threads, they form a new thread whose thickness corresponds to the sum of the individual thicknesses. The slope becomes the average of the two slopes.*

4.1.2 Analysis

The model as described above results in the fairly regular behaviour seen in Figure 4.1. Note that time evolves downwards and the initial configuration can be seen in the top row. An immediate observation is that all threads seem to merge at the same time in groups of either 3 or 2 threads. The resulting threads of thickness 3 then merge to form thickness 6. This behaviour bears some differences to the CA which it should model since the simultaneous merging of 3 threads has not been observed before and 6 is not a Fibonacci number. We can already contemplate whether the model resulting directly from Definition 4.4 is the right model.

Nonetheless, let us first look at how this behaviour emerges and specifically examine under what circumstances 3 threads merge simultaneously so that a new toy model which does not exhibit this property can be crafted. To understand which threads will merge, it helps to calculate the differences in slopes. For this system, the first few slopes will be

$$\{\varphi\},\ \{2\varphi\},\ \{3\varphi\},\ \{4\varphi\},\ \{5\varphi\} = \varphi - 1,\ 2\varphi - 3,\ 3\varphi - 4,\ 4\varphi - 6,\ 5\varphi - 8,$$

[1] We will examine these properties in more depth by looking at phyllotaxis patterns in Section 4.2. But for now, let us explore this first system without much formality.

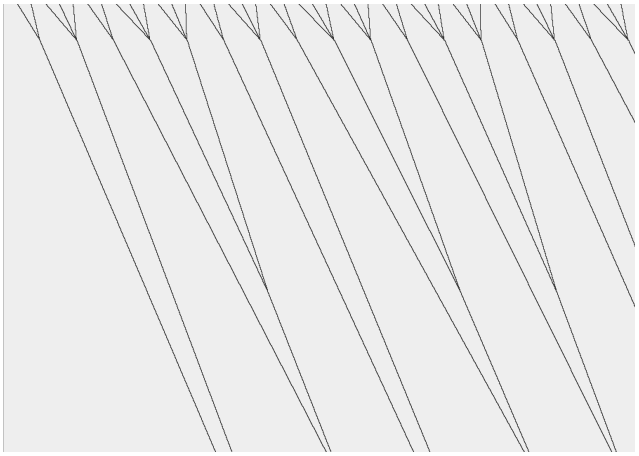

Figure 4.1: The golden ratio slope system results in the depicted merging and evolution of threads.

where we replace $k\varphi$ with $k\varphi - \lfloor k\varphi \rfloor$ to obtain its fractional part. We note that the sequence $\lfloor k\varphi \rfloor$ is the *Lower Wythoff Sequence* as found in the OEIS[2] [16]:

Definition 4.5 *The* Lower Wythoff Sequence *is a Beatty sequence (cf. Definition 2.11) with* $a_n = \lfloor n\varphi \rfloor$. *The sequence begins with* 1, 3, 4, 6, 8, 9, 11, ...

Its complement is the Beatty sequence with $\beta = \varphi^2$, also known as the *Upper Wythoff sequence*. Interestingly, these Beatty sequences were proven to be the set of safe combinations for (non-blocking) Wythoff Nim in [20].

Now we are well equipped to compute the differences between consecutive slopes:

$$\varphi - 2,\ \varphi - 1,\ \varphi - 2,\ \varphi - 2,\ \varphi - 1,\ \ldots$$

In the following, we show that these are the only two differences in the first layer. For some $\alpha, \beta \in [0, 1)$ the kth difference is

$$\begin{aligned}(k\varphi - \lfloor k\varphi \rfloor) - ((k-1)\varphi - \lfloor (k-1)\varphi \rfloor) &= \varphi + \lfloor (k-1)\varphi \rfloor - \lfloor k\varphi \rfloor \\ &= \varphi + ((k-1)\varphi - \alpha) - (k\varphi - \beta) \\ &= \varphi + (-\varphi - \alpha + \beta)\end{aligned}$$

Note that $\lfloor (k-1)\varphi \rfloor - \lfloor k\varphi \rfloor$ is an integer, and therefore the terms below it must also be integers. Specifically, $(-\varphi - \alpha + \beta)$ is an integer and must be greater than $-\varphi - 1$ and less than $-\varphi + 1$. Since it cannot be zero for the given α and β, it must be in the set $\{-2, -1\}$. Therefore, the kth difference must be $\varphi - 2$ or $\varphi - 1$ for all k.

[2]The On-Line Encyclopedia of Integer Sequences is a comprehensive database containing many integer sequences.

Looking at the patterns of threads, we detect that whenever the difference $\varphi - 2$ appears twice in a row, three threads merge. Therefore the sequence of 2s and 1s is directly related to the merging process. We will make use of this observation to develop the final toy model.

Empirical Studies of Various Parameters

Following the basic definition of the model which does not seem to be quite correct yet, a modified version could produce the desired result or at least better results. We made a few observations by tweaking the model's initial slopes as well as the merging process. First, similar parameters for the slope multiples were run through the program. Second, a different average of the merged slopes was taken by computing the weighted average.

To begin the search for slope parameters, let us remark that $\{\varphi^2\} = \{(\varphi + 1)n\} = \{\varphi n\}$, so taking this power of φ as well as adding any integer to it will not change the fractional part. We thus need to look into other areas of possible parameters. Since our observations above led us to a Beatty sequence which provides P-positions for Wythoff Nim, we will look at various similar sequences, which were also mentioned in the paper containing the proof for Wythoff Nim [20]. The first pair bearing similar properties is $\{k\sqrt{2}\}$ and $\{k(2+\sqrt{2})\}$. Considering that we take the fractional part of the resultant Beatty sequence, we only test the output of one sequence of the pair (the output for both sequences is the same). As a next pair, we consider the complementary Beatty sequences $\{k\frac{\sqrt{13}-1}{2}\}$ and $\{k\frac{\sqrt{13}+5}{2}\}$. And lastly, we examine the Beatty sequence generated by $\{k\sqrt{5}\}$ since $\sqrt{5}$ is directly linked to the golden ratio.

In Table 4.1, the results are summarized by showing the percentage of final threads having a Fibonacci number as their thickness, for $n = 1$ to 100 starting threads. In the first column, we can see the original slope system (cf. Definition 4.4). The *random* parameter was derived by creating a random `double` r for every number n of starting threads and then computing the initial slopes as $\{k \cdot r\}$, similar to the other parameters. We observe that the golden ratio multiples outperform the other parameters concerning the number of Fibonacci numbers produced. Additionally, the other Beatty sequences provided inferior parameters, also when compared to random initial slopes. Considering the close link between Fibonacci numbers and the golden ratio, we can consider this a reasonable result.

Let us now shift the focus away from tweaking the initial slopes and consider various methods of merging the slopes. Since multiples of φ provided the best results in the parameter search, we will only consider these as initial slopes. We consider two different weights for the average: thread thickness and index. One could argue for a thread of higher thickness to have merged

Initial slopes	$\{k\varphi\}$	$\{k\sqrt{2}\}$	$\{k\frac{\sqrt{13}-1}{2}\}$	$\{k\sqrt{5}\}$	*random*
Fibonacci numbers	76.54%	56.43%	28.57%	65.02%	69.98 %

Table 4.1: Percentage of Fibonacci numbers in the thicknesses of the final threads after $10,000$ iterations of the program. Various parameters for the initial slopes are tested, with random parameters and the original slopes as a comparison.

Average type	normal	weighted by thickness	weighted by index
Fibonacci numbers	76.54%	90.98%	80.93%

Table 4.2: Percentage of Fibonacci numbers in the thicknesses of the final threads after $10,000$ iterations of the program. The initial slopes are as in Definition 4.4 and various average computations for the merging of slopes are tested (we refer to the computer program [1] for how this was implemented).

with more threads in the past and thus be more important. We also choose weights by indices since it was empirically observed that when three threads merge simultaneously, weighting the first two threads higher yields better results (consider also Appendix B for more information). Viewing Table 4.2, two conclusions can be drawn: Firstly, a weighted average is favourable over a standard average and secondly, weighting by thickness generates the most Fibonacci numbers.

Finally, we conclude that the best results could be produced by multiples of the golden ratio modulo 1 (i.e., the fractional part) and using a weighted average by thickness. However, we refer to Appendix B for one last study of an intriguing discovery which also shows that this toy model is not the sought-after one.

4.2 Phyllotaxis

In this section, we look at possible parameters for the toy system from a slightly different angle. That is, we look at phyllotaxis patterns to derive some useful properties about the golden ratio and its relation to Fibonacci and Lucas numbers.[3] Phyllotaxis refers to the outwards growing arrangement of leaves in plants. Most famous are the patterns of pineapple fruit and sunflower seeds, in both of which the Fibonacci numbers naturally appear. We can use phyllotaxis to analyse integer multiples of irrational numbers, in our case to look at Fibonacci and Lucas number multiples of the golden ratio or related parameters. For our purposes of examining the relationships between the golden ratio, Fibonacci numbers and Lucas numbers, we define the following form:

[3]Phyllotaxis has also been studied with regard to Wythoff's game, and a work linking all of these concepts can be found in [6].

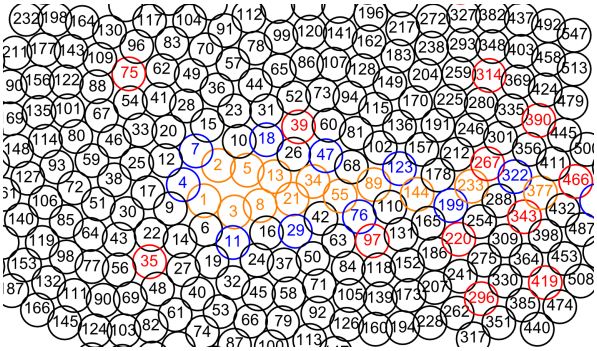

Figure 4.2: An excerpt of the phyllotaxis pattern generated by Definition 4.6. Fibonacci numbers are coloured orange and Lucas numbers blue. In red we see values of k for which central region of the blocking queens CA empirically looks a certain way.

Definition 4.6 *We consider dots (depicted as the number N in a circle) on the polar plane. The Nth dot is placed at position* $(\sqrt{N}, 2\pi N \cdot \frac{1}{\varphi})$ *and the phyllotaxis pattern is generated by all these dots.*

Figure 4.2 shows the pattern generated by Definition 4.6.[4] Note that this is a rectangular image but the phyllotaxis pattern would normally evolve in an approximately circular motion, hence the missing dots around the borders can be ignored. It can be seen that the Fibonacci and Lucas numbers, highlighted in orange and blue respectively, stay more or less around the zero-angle axis. When looking at this pattern for even higher numbers, they seem to stray from the axis within increasingly smaller bounds. As we will see later in Theorem 4.8 and Theorem 4.9, this can be proven and unveils interesting facts about the number sequences.

The phyllotaxis patterns exhibit several properties of interest. Following, we prove some properties related to the Lucas and Fibonacci numbers in the hopes of finding parameters which could be useful for the slope system.

Proposition 4.7 *The patterns generated by* $(\sqrt{N}, 2\pi N \cdot \frac{1}{\varphi})$ *and* $(\sqrt{N}, 2\pi N\varphi)$ *are the same.*

This first property follows directly from a well-known property of φ: $\varphi = 1 + \frac{1}{\varphi}$. So when we multiply $1 + \frac{1}{\varphi}$ by $2\pi N$ we get the same result as for $\frac{1}{\varphi}$, since $2\pi N$ has angle zero in the polar plane for any integer N.

Next, we examine Fibonacci and Lucas numbers with the help of phyllotaxis patterns. As can be observed in Figure 4.2 and hinted above, Fibonacci and Lucas numbers lie close to the axis. This finding can be proven by considering the definition of the number sequences from Section 2.3.1.

[4] We thank Dr. Matthew Cook for providing this and the other phyllotaxis graphic (cf. Figure 4.3).

Theorem 4.8 *The Fibonacci numbers lie near the zero-angle axis in the pattern generated by* $(\sqrt{N}, 2\pi N \cdot \frac{1}{\varphi})$.

Proof Note that to prove this statement it suffices to show that Fibonacci numbers approximate integer multiples of φ. Following, we show that F_{n+1} approximates $F_n\varphi$ and thus F_{n+1} generates points near $(\sqrt{F_{n+1}}, 2\pi \cdot \frac{F_n\varphi}{\varphi}) = (\sqrt{F_{n+1}}, 2\pi \cdot F_n)$ which lie at the zero-angle axis since the angle is an integer multiple of 2π.

As in Definition 2.7, let $\overline{\varphi} = \frac{1-\sqrt{5}}{2} = 1 - \varphi$. Then

$$\begin{aligned} F_n\varphi - F_{n+1} &= \frac{\varphi^n - \overline{\varphi}^n}{\sqrt{5}} \cdot \varphi - \frac{\varphi^{n+1} - \overline{\varphi}^{n+1}}{\sqrt{5}} \\ &= \frac{-\varphi \cdot \overline{\varphi}^n + \overline{\varphi}^{n+1}}{\sqrt{5}} \\ &= \overline{\varphi}^n \cdot (-1) \\ &= -\left(\frac{-1}{\varphi}\right)^n \end{aligned}$$

It follows that $|F_n\varphi - F_{n+1}| = \left(\frac{1}{\varphi}\right)^n$. Since $\frac{1}{\varphi} < 1$, $\left(\frac{1}{\varphi}\right)^n$ is an exponentially decreasing sequence and we can conclude that F_{n+1} approximates an integer multiple of φ. Therefore F_{n+1} and any other Fibonacci number lie close to the zero-angle axis. □

We note that this proof involves the closed formula for Fibonacci numbers (cf. Equation 2.1). In Appendix A, an alternative proof that only uses the recurrence equation is shown.

We can observe a similar property for the Lucas numbers:

Theorem 4.9 *The Lucas numbers lie near the zero-angle axis in the pattern generated by* $(\sqrt{N}, 2\pi N \cdot \frac{1}{\varphi})$.

Proof Similar to the proof of Theorem 4.8, we show that L_{n+1} approximates $L_n\varphi$.

$$\begin{aligned} |L_n\varphi - L_{n+1}| &= |\,(\varphi^n + \overline{\varphi}^n) \cdot \varphi - \left(\varphi^{n+1} + \overline{\varphi}^{n+1}\right)\,| \\ &= |\overline{\varphi}^n\varphi - \overline{\varphi}^{n+1}| \\ &= |\overline{\varphi}^n \cdot \sqrt{5}| \\ &= \sqrt{5} \cdot \frac{1}{\varphi^n} \end{aligned}$$

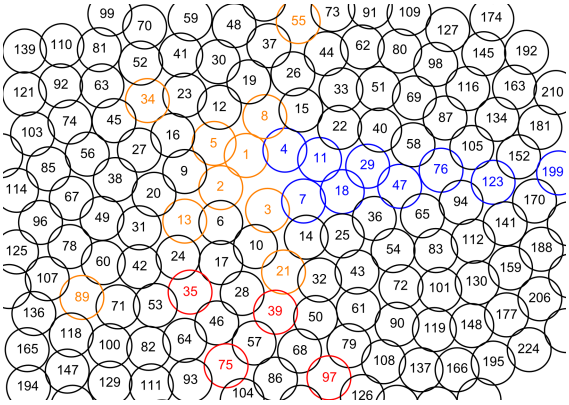

Figure 4.3: An excerpt of the phyllotaxis pattern generated by Definition 4.6, but where the Nth dot is at $(\sqrt{N}, 2\pi N \cdot \frac{1}{\varphi+2})$. Fibonacci numbers are coloured orange and Lucas numbers blue. In red we see values of k for which central region of the blocking queens CA empirically looks a certain way.

Again, we have the same exponentially decreasing sequence, where the factor of $\sqrt{5}$ can safely be ignored as constant. It follows that also L_{n+1} approximates an integer multiple of φ and the Lucas numbers lie near the zero-angle axis. □

A corollary which follows almost immediately goes as follows:

Corollary 4.10 *Both the Fibonacci and Lucas numbers lie near the zero-angle axis in the pattern generated by* $(\sqrt{N}, 2\pi N \cdot \frac{1}{\varphi+1})$.

Proof Following, we show the derivation for the Fibonacci numbers. Since the Lucas numbers satisfy the same recurrence relation, a very similar argumentation also holds.

$$\begin{aligned} |F_n(\varphi+1) - F_{n+2}| &= |F_n\varphi + F_n - (F_n + F_{n+1})| \\ &= |F_n\varphi - F_{n+1}| \\ &= \frac{1}{\varphi^n} \end{aligned}$$

By the same argument as above, this proves the corollary. □

The next theorems show us an interesting property of $\varphi + 2$, that is, the Fibonacci and Lucas numbers are placed along different axes. Consider Figure 4.3 to verify that Lucas numbers (in blue) lie near the axis, whereas Fibonacci numbers (in orange) are spread along four axes. Recall from Section 2.3.1 that it has been empirically observed in the CA that adding a large Lucas number does not change the behaviour of the inner sector whereas adding a Fibonacci number does. Therefore the parameter $\varphi + 2$ might be related to the cellular automaton.

Theorem 4.11 *The Lucas numbers lie near the zero-angle axis in the pattern generated by* $(\sqrt{N}, 2\pi N \cdot \frac{1}{\varphi+2})$.

Proof We approach this with continued fraction approximations as seen in Section 2.3.2. Let us now derive the continued fraction of $\varphi + 2$.

$$\varphi + 2 = 3 + \frac{1}{\varphi} = 3 + \cfrac{1}{1 + \cfrac{1}{1 + \cdots}}$$

Its convergents are $\frac{3}{1}, \frac{4}{1}, \frac{7}{2}, \frac{11}{3}, \frac{18}{5}, \frac{29}{8}$. We observe that the nth term corresponds exactly to $\frac{L_{n+2}}{F_{n+1}}$. Applying Theorem 2.17, we get:

$$|F_{n+1}(\varphi + 2) - L_{n+2}| \leq \frac{1}{F_{n+2}} \tag{4.1}$$

Since $\frac{1}{F_{n+2}}$ is an exponentially decreasing sequence, L_{n+2} approximates $F_{n+1}(\varphi + 2)$. This is an integer multiple of $\varphi + 2$ and thus the Lucas numbers lie near the axis. □

Now we can look at one final property of phyllotaxis patterns which we prove. Again, we consider the pattern generated by $\varphi + 2$, but this time with the Fibonacci numbers and unveil a surprising result.

Theorem 4.12 *In the pattern generated by* $(\sqrt{N}, 2\pi N \cdot \frac{1}{\varphi+2})$*, the Fibonacci numbers lie near one of four directions not close to the zero-angle axis.*

Proof We approach this proof by showing that $\frac{5F_n}{\varphi+2}$ is not a multiple of 5, which results in the conclusion that $\frac{F_n}{\varphi+2}$ is not an integer. If we can further show that all other modulo 5 values are results of $\frac{5F_n}{\varphi+2}$, this will prove that $\frac{F_n}{\varphi+2}$ lies in one of four directions corresponding to the modulo values.

By Equation 4.1,

$$|F_{n-1}(\varphi + 2) - L_n| + 2 \cdot |F_n(\varphi + 2) - L_{n+1}| < \frac{1}{F_n} + \frac{2}{F_{n+1}} \tag{4.2}$$

Note that

$$\begin{aligned}(F_{n-1}(\varphi + 2) - L_n) - 2(F_n(\varphi + 2) - L_{n+1}) \leq \\ |F_{n-1}(\varphi + 2) - L_n| + 2 \cdot |F_n(\varphi + 2) - L_{n+1}|\end{aligned} \tag{4.3}$$

So we can replace (4.2) with

$$(2L_{n+1} - L_n) - (2F_n - F_{n-1}) \cdot (\varphi + 2) < \frac{1}{F_n} + \frac{2}{F_{n+1}} \tag{4.4}$$

Using the formula from Equation 2.3, we can see that

$$2F_n - F_{n-1} = F_n + F_{n-2} = L_{n-1}$$

Thus (4.4) becomes

$$(2L_{n+1} - L_n) - L_{n-1}(\varphi + 2) < \frac{1}{F_n} + \frac{2}{F_{n+1}} \tag{4.5}$$

With increasing n, the right-hand side of this inequality grows smaller. So it follows that $2L_{n+1} - L_n$ approximates $L_{n-1}(\varphi + 2)$.

Similarly, if we divide by $\varphi + 2$, we get

$$\frac{2L_{n+1} - L_n}{\varphi + 2} - L_{n-1} < \left(\frac{1}{F_n} + \frac{2}{F_{n+1}}\right) \cdot \frac{1}{\varphi + 2} \tag{4.6}$$

where we can again consider the right-hand side to grow small for large n. We can use the formula from Equation 2.4 to substitute

$$\frac{2L_{n+1} - L_n}{\varphi + 2} = \frac{5F_n}{\varphi + 2}$$

And therefore (4.6) becomes

$$\frac{5F_n}{\varphi + 2} - L_{n-1} < \left(\frac{1}{F_n} + \frac{2}{F_{n+1}}\right) \cdot \frac{1}{\varphi + 2} \tag{4.7}$$

Or, in other words, for sufficiently large n, L_{n-1} can be said to approximate $\frac{5F_n}{\varphi + 2}$. And finally, we remark that the Lucas numbers (including L_{n-1}) modulo 5 follow the repetitive pattern $2, 1, 3, 4, 2, \ldots$ and thus a Lucas number is never $0 \pmod 5$. This shows that $\frac{5F_n}{\varphi + 2}$ has the values $2, 1, 3, 4, 2, \ldots \pmod 5$ and if we divide by 5 to compute the different angles in the phyllotaxis pattern, we obtain four different fractions of an integer, corresponding to the four directions. □

4.3 Final Slope System

In this section, we derive the final toy model and examine its properties. Drawing on the findings of Section 4.1.2, we can summarize:

1. The differences in the slopes were fairly regular and seemed to predict whether two or three threads merge.
2. The golden ratio provided the best parameter for taking multiples, so we can empirically rule out any other parameters for now.
3. The weighted average by thickness gives the best results.

We observed that the difference $\{(k+1)\varphi\} - \{k\varphi\}$ is either $\varphi - 2$ or $\varphi - 1$. Note that the sequence of these differences seems to follow a regular pattern of 2's and 1's. This leads us to the discovery of a new sequence which provides the initial slopes for the model in this section.

4.3.1 Model Definition

Definition 4.13 *In the initial configuration, there are n threads where the kth thread has initial slope* $s_k = \lfloor k\varphi \rfloor - \lfloor (k-1)\varphi \rfloor$ *and thickness* $t_k = 1$.[5] *We write the slopes as fractions* $s_k = \dfrac{n_k}{d_k}$. *When two threads with slopes* s_t *and* s_q *merge, the resulting slope is* $\dfrac{n_t + n_q}{d_t + d_q}$ *and the thickness is* $t_t + t_q$.

Observe that the new slope of merged threads corresponds exactly to the average of their slopes weighted by thickness since the thickness is given by the denominators d_k. The initial thicknesses are 1 and they add when merging, just like the denominators.

In Figure 4.4, we can see how the threads evolve and merge. In the top row, the initial configuration is shown. It can be observed that the merging happens in simultaneous steps, similar to the golden ratio slope system. However, only two threads merge at a given time (which correlates more with observations of the cellular automaton) and we do not see any merging to non-Fibonacci numbers.

4.3.2 Analysis

Let us first look at the initial slopes. We remark that the slopes s_k are always either 1 or 2 and write down the first few slopes:

$$2,\ 1,\ 2,\ 2,\ 1,\ 2,\ 1,\ 2,\ \ldots \tag{4.8}$$

One can now see that this sequence follows the recursion

$$s_n = s_{n-1},\ s_{n-2}$$

[5] Notice that the initial slopes are defined by differences of successive terms of the lower Wythoff sequence (cf. Definition 4.5)

Figure 4.4: An image of the first few iterations of the final model. The threads behave as in Definition 4.13 and time evolves downwards.

with $s_0 = 2$ and $s_1 = 2,\ 1$.[6]

Definition 4.14 *We define the sequence S derived from the slopes and a parameter θ as follows: S_k is 0 if slope $s_k > \theta$ and 1 if $s_k \leq \theta$.*

Example 4.15 *For this toy model, the initial slopes seen in Equation 4.8 in combination with the parameter $\theta = \varphi$ result in the sequence S of*

$$0,\ 1,\ 0,\ 0,\ 1,\ 0,\ 1,\ 0,\ \ldots \tag{4.9}$$

This sequence is known as *the infinite Fibonacci word* (sequence A003849 in the OEIS) and can also be obtained by swapping 2 with 0 in Equation 4.8. The infinite Fibonacci word is morphic (i.e., has a mapping to itself), and applying the rule $0 \to 01,\ 1 \to 0$ results in the same sequence again. It can be seen that the merging process also seems to follow a set of replacement rules. For example, in the first iteration, every thread of slope 2 followed directly by a thread of slope 1 merges into the thread of slope 1 from the left. Figure 4.5 shows the first iterations in terms of the slopes and the resulting sequences generated. Note that the second row of Figure 4.5b corresponds to the infinite Fibonacci word with 0 and 1 flipped. Next, the third row is the Fibonacci word with a 1 added to the beginning. Subsequently, these two steps repeat themselves.

[6] We separate the numbers by commas to clarify that we are *concatenating* and not adding them, but the commas could also be omitted.

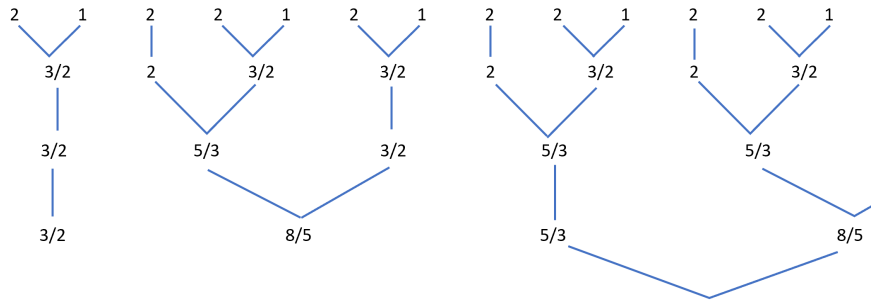

(a) The first merging steps of the final toy model including the slopes of all threads.

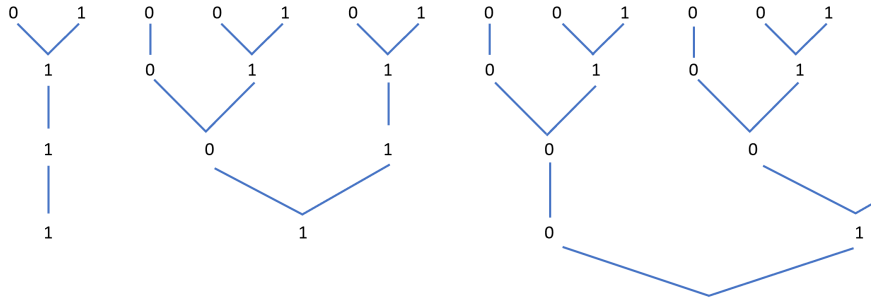

(b) The resulting sequence defined by comparisons to the golden ratio (cf. Equation 4.9), generated by the graphic above.

Figure 4.5: The initial merging steps where the slopes are written numerically at the top and as a simplified sequence at the bottom.

We stipulate that the slopes in the final toy model always correspond to fractions $\frac{F_{n+1}}{F_n}$, where the denominator F_n corresponds to the thickness of a given thread. Since ratios of Fibonacci numbers are the convergents of the continued fraction of the golden ratio (cf. Example 2.14), it follows that φ must lie between two successive ratios and the slopes alternatively over- and under-approximate the golden ratio. Equivalently, the sequence of Definition 4.14 with the parameter $\theta = \varphi$ will flip from 0 to 1 and vice versa in every merging step. After two steps of merging, the sequence will have flipped twice and thus be the same again. Following this argumentation, one can see that the merging repeatedly follows the same pattern of these two steps, incrementing numerators and denominators of the slopes to the next Fibonacci numbers.

In the following, we formalise this argument in a proof that the thicknesses of the threads always correspond to Fibonacci numbers. Moreover, we show the stronger statement that the slopes are fractions of successive Fibonacci numbers (note that by definition of the model, the denominators denote

thread thicknesses).

Proof We prove the following statement by induction on the number of merging steps: Given that we have threads with slopes $\frac{F_{n+1}}{F_n}$ and $\frac{F_{n+2}}{F_{n+1}}$ after $n-1$ steps of merging, where $\frac{F_{n+1}}{F_n} \leq \varphi$ and $\frac{F_{n+2}}{F_{n+1}} > \varphi$ and the slopes give rise to the sequence shown in Example 4.15. After two more steps of merging, the resulting slopes give rise to the same sequence as before with a 1 prepended and are ratios $\frac{F_{n+3}}{F_{n+2}}$ and $\frac{F_{n+4}}{F_{n+3}}$.

Base Case: In the first row, all slopes are either $\frac{F_2}{F_1} = 1 \leq \varphi$ or $\frac{F_3}{F_2} = 2 > \varphi$. After the first merging step, we get $2, 1 \to 3/2$ and $2/1 \to 2/1$ as a slope transformation. Note that $2 > \varphi$ and $3/2 \leq \varphi$, so the resulting sequence would be

$$1, 0, 1, 1, 0, 1, 0, 1, 1, 0, \ldots$$

This is the same sequence with the symbols 1 and 0 swapped. After another step of merging where $2, 3/2 \to 5/3$ and $3/2 \to 3/2$, we obtain

$$1, 0, 1, 0, 0, 1, 0, \ldots$$

and are therefore back at the original sequence with a 1 prepended and the slopes modified to ratios of $\frac{F_4}{F_3} = \frac{3}{2} \leq \varphi$ or $\frac{F_5}{F_4} = \frac{5}{3} > \varphi$.

Induction Step: Looking at the sequence in Equation 4.9, we can see that the ones represent slopes of $\frac{F_{n+1}}{F_n}$ and the zeroes are for slopes of $\frac{F_{n+2}}{F_{n+1}}$ after $n-1$ steps of merging. Since threads with higher slopes merge into threads with lower slopes, the resulting sequence after one merging step is

$$1, 0, 1, 1, 0, 1, 0, 1, 1, 0, \ldots$$

where the ones are the result of merging $\frac{F_{n+1}}{F_n}$ and $\frac{F_{n+2}}{F_{n+1}}$ into a thread of slope $\frac{F_{n+1} + F_{n+2}}{F_n + F_{n+1}} = \frac{F_{n+3}}{F_{n+2}}$, which is less than the golden ratio (since it is the next convergent in its continued fraction). Another merging step yields

$$1, 0, 1, 0, 0, 1, 0, \ldots$$

and the slopes are $\frac{F_{n+4}}{F_{n+3}}$ (denoted by 0 and the result of merging 0 and 1) and $\frac{F_{n+3}}{F_{n+2}}$ from before. □

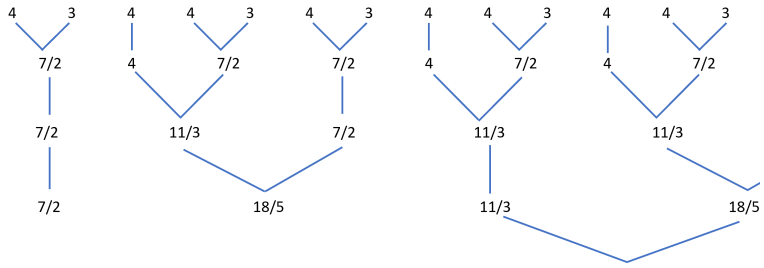

Figure 4.6: The slopes produced by the first few iterations of a toy model which produces Fibonacci thicknesses but has the Lucas numbers in its numerators. Note that the same sequence as in Figure 4.5b could be drawn by comparing the slopes to $\varphi + 2$.

4.3.3 Alternative Models

After examining this slope system more closely, we can note that its behaviour arises from two main properties:

1. The initial slopes are chosen as some simple mapping of the infinite Fibonacci word, where $0 \to x$ and $1 \to y$ such that x and y are some integers satisfying $x > y$.
2. The slopes after one step of merging result in the infinite Fibonacci word with 0 and 1 exchanged and after two steps of merging they yield the same sequence S from Definition 4.14 with a 1 prepended.

For any of these models, the numerators are members of the generalised Fibonacci sequence and the denominators are Fibonacci numbers since they both follow the same recursion and all initial thicknesses are chosen to be 1 (satisfied by the requirement that x and y are integers).

Consequently, we can define a series of other toy models that satisfy the same merging property. Let us look at one model which produces fractions $\frac{L_{n+2}}{F_{n+1}}$ as slopes. Consider Figure 4.6 to see the evolution of the first few slopes. The initial slopes are defined by applying the mapping $0 \to 4$ and $1 \to 3$ of the infinite Fibonacci word. This results in the sequence

$$s_k = \lfloor k(\varphi + 2) \rfloor - \lfloor (k-1)(\varphi + 2) \rfloor$$

of initial slopes. Note that this sequence corresponds to the differences in successive terms of the Beatty sequence produced by $\varphi + 2$.

By observing the first few merging steps, it becomes evident that the numerators start with L_2 and L_3 and continue following Lucas' recursion whereas the denominators follow the same pattern as the toy model from before. We can construct a proof showing that this model indeed also satisfies the two properties mentioned above. Notice that the slopes seem to converge

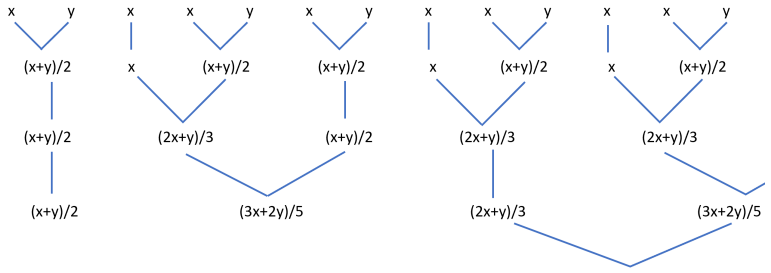

Figure 4.7: The slopes produced by the first few iterations of a generalised toy model which produces Fibonacci thicknesses. The integers x and y are chosen such that $x > y$ and give rise to the generalised Fibonacci sequence in the numerators.

to $\varphi + 2$, so the sequence from Definition 4.14 can be set out for $\theta = \varphi + 2$. Following, we state how it could be proven that the fractions of the slopes are alternatively greater than and less than this number.

From the proof of Theorem 4.11, we know that the continued fraction of $\varphi + 2$ has $\dfrac{L_{n+2}}{F_{n+1}}$ as its nth convergent. Now the statement can be proven analogously to the proof for the toy model from before by replacing φ with $\varphi + 2$ and choosing the respective fractions of Lucas and Fibonacci numbers. Since the proof would follow the same steps, we omit it here.

We conclude that the toy model for $\varphi + 2$ is one of a class of possible toy models which are defined in the same way. Essentially, the same sequence of any two numbers could be chosen to satisfy the two properties listed at the beginning of this section. Note that the requirement that $x > y$ results in the first merged slope satisfying $\dfrac{x+y}{2} < x$, so x will merge into the merged thread from the left (cf. Figure 4.7).

Chapter 5

Future Work

In this chapter we will apply the findings of Chapter 4 and continue the analysis of the warp of the cellular automaton, providing an outlook for further research. As we saw in Section 2.2.1, the warp of the CA is a symmetric region dominated by yellow threads. Using the toy model, we could successfully model the behaviour of these threads and also provide some insight into the origins of this behaviour. Yet, we did not look into the regions between threads which are dominated by black and blue vertical or diagonal lines (cf. Figure 2.3).

5.1 Vertical Blue Densities

Let us now examine the mostly blue and black regions between yellow threads. For this purpose, we recap the colour scheme used in [5], where the colours signify the number of P-positions (palaces) visible minus the blocking number k. Using the same terminology as the paper defining the CA, we call this number the *surplus number* [5]. Now we can set the colours

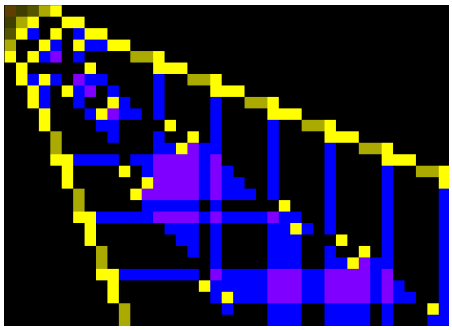

Figure 5.1: The beginning of Game 5 ($k = 5$) to visualize the colouring of winning and losing positions.

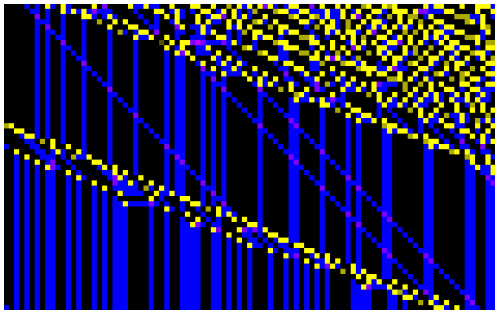

(a) The blue, black and purple region in-between the threads of Game 68.

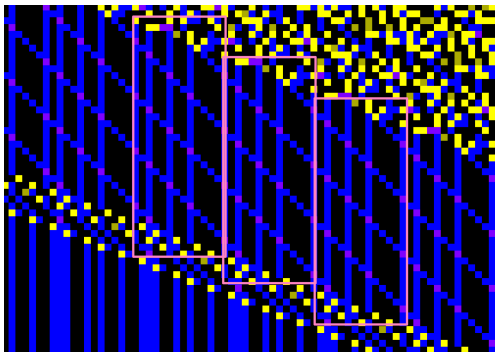

(b) The blue, black and violet region in-between the threads of Game 68, once the warp has become periodic. Three steps of the repetitive pattern are highlighted in pink.

Figure 5.2: A comparison of the region between threads of Game 68. At the top, we see it early in the game and at the bottom in a later stage once the behaviour has become periodic.

for the respective surplus numbers: -2 = Light Olive, -1 = Yellow, 0 = Black, 1 = Blue, 2 = Indigo (violet). Negative numbers (depicted by yellowish colours) resemble P-positions as the player moving to one of these positions can block all P-positions seen from there. Similarly, positive numbers, seen in hues of blue, denote losing moves. Apart from the yellow threads, only blue, black and some purple positions are observable in the warp.

We observe that in Figure 5.1, the warp region above the inner sector (using the terminology described in Figure 2.2) contains a single blue vertical line, followed by four black vertical lines, once the pattern becomes periodic (this happens quite fast, starting at column 14 when counting from the left). The yellow dots appear only after a black vertical line. Therefore we note a 20% *vertical density* of blue for $k = 5$ blocking positions.

Considering a more complex game with $k = 68$, the pattern becomes periodic much later and we can notice three blue threads with the occasional violet

cell in Figure 5.2a.[1] We observe that whenever a blue diagonal and vertical line cross, a violet position appears. This can be explained by calculating the corresponding value in the cellular automaton and verifying that it is 2, for the update rule, we refer to [5]. Similar to game 5, we can compute a vertical density of blue threads, which is $4/13$ for Game 68.

Furthermore, by looking at the periodic warps generated by other values of k below 100 (for higher k, it takes a long time for the patterns to converge, but probably similar observations could be made), the same pattern as highlighted in Figure 5.2b appears several times as well. Noting that every block of black lines is intercepted by exactly one blue vertical line, we can abbreviate this pattern by the vertical thicknesses of black threads as $(1,2,2,4)$. We also noticed the patterns $(4,1,5)$ (resulting in a blue vertical density of $3/13$), $(3,2,5)$ (resulting in the same blue vertical density) and $(1,2,1,5)$ (resulting in $4/13$). These observations are not conclusive, however, they hint toward a more general rule for the blue and black threads. We remark that the thickness of the last black thread was found to be equal to the sum of the previous two or three threads in these examples and the blue densities seem to stay roughly the same.

5.2 Outlook

The empirical analysis of the blue and black regions between yellow threads in Section 5.1 provides some insight into the warp for several k. We note that they are early findings and not yet generalised properties which apply to all k. The warp remains a region for which convergence to periodicity seems unpredictable and differs even for similar blocking numbers. Future research could provide general formulae for the pattern of blue and black threads, starting by defining a comprehensive list of these repetitive blocks of black threads mentioned above. Similar to our analysis of the yellow threads and their thicknesses, the black and blue thicknesses could also be related to certain number sequences.

[1] We did not choose 68 for any particular reason other than that it is a higher number of blocking positions while still becoming periodic within a reasonable number of steps.

Chapter 6

Conclusion

In this thesis, we analysed a substructure (called the warp) of the cellular automaton for blocking queen games proposed in [5]. We have come up with a toy model which exhibits the same merging property as the cellular automaton and provided a generalised version of it. The study of the golden ratio and its closely related number sequences, the Fibonacci and Lucas numbers, provided the mathematical framework for this toy model. The model provides some regularity and predictability to the largely unexplored and chaotic nature of the palaces in k-blocking Wythoff Nim. Understanding the number sequences which dictate the behaviour of P-positions in the warp may lead to a better understanding of the CA in general and provide a basis for future research into k-blocking Wythoff Nim. The main contributions of this work are

- We closely examined the behaviour of threads of palaces in the warp and set out the requirements for a toy model.
- A first toy model, called the "golden ratio slopes system" was analysed with the help of a program. We extracted some important mathematical properties to continue the search for a better-suited toy model.
- Following up on early findings from the golden ratio slopes system, we analysed phyllotaxis patterns generated by various parameters and identified some differences between the Lucas and Fibonacci numbers.
- This has led to the discovery of a functioning final toy model, which could then be generalised. We study two versions of this system whose slopes converge to φ and $\varphi + 2$ respectively.

Remarkably, not only one but a series of functioning toy models closely related to the infinite Fibonacci word could be found. This also points towards the limitations of such a toy model as it can only represent the behaviour of the cellular automaton within its requirements. Without a

further study of the warp's properties, we cannot determine the "best" toy model of its class. Further analysis of the CA's complex behaviour, especially with regard to the disconnected threads and the mostly blue and black regions between them could provide more insight into the early empirical observations which we provided in Chapter 5. More generally, it would be interesting to be able to relate the initial slopes and the repetitive slope merging process in the toy model to the blocking queen game.

Appendix A

Alternative Proof of Theorem 4.8

We provide an alternative proof of Theorem 4.8 using continued fractions here for the sake of completeness and since it shows a property of fractions of Fibonacci numbers (which appear in the final toy model as well). The proof might be less elegant, yet, is very simple and follows from the recursive definition of the Fibonacci numbers (thus the same argument could be used for the Lucas numbers and any other related sequence). Before we begin with the proof, we state a lemma which will be useful later.

Lemma A.1 *For any Fibonacci number F_n,*

$$F_{n+2} \cdot F_n - (F_{n+1})^2 = \pm 1.$$

Proof We proceed by induction on n. Base Case $(n = 1)$

$$F_3 \cdot F_1 - (F_2)^2 = 2 \cdot 1 - 1^2 = 1$$

Inductive step $(n \longrightarrow n+1)$

$$\begin{aligned} F_{n+2} \cdot F_n - (F_{n+1})^2 &= (F_n + F_{n+1})F_n - (F_{n+1})^2 \\ &= F_n^2 + F_n \cdot F_{n+1} - F_{n+1}(F_n + F_{n-1}) \\ &= F_n^2 - F_{n+1} \cdot F_{n-1} \\ &= \pm 1 \end{aligned}$$

Where, in the last step, we used the induction hypothesis. □

For the reader's convenience, we state the theorem again:

Theorem A.2 *The Fibonacci numbers lie near the zero-angle axis in the pattern generated by $(\sqrt{N}, 2\pi N \cdot \frac{1}{\varphi})$.*

Proof Recall from Example 2.14 that the kth convergent of the continued fraction of the golden ratio is $\frac{F_{k+1}}{F_k}$. In consequence, φ must lie between successive convergents, that is

$$\frac{F_{k+1}}{F_k} < \varphi < \frac{F_{k+2}}{F_{k+1}}.$$

Or, equivalently,

$$0 < \varphi - \frac{F_{k+1}}{F_k} < \frac{F_{k+2}}{F_{k+1}} - \frac{F_{k+1}}{F_k} \tag{A.1}$$

Further,

$$\frac{F_{k+2}}{F_{k+1}} - \frac{F_{k+1}}{F_k} = \frac{F_{k+2} \cdot F_k - (F_{k+1})^2}{F_k \cdot F_{k+1}}$$

Following Lemma A.1,

$$\left| \frac{F_{k+2} \cdot F_k - (F_{k+1})^2}{F_k \cdot F_{k+1}} \right| = \frac{1}{F_k \cdot F_{k+1}}.$$

We can insert this into (A.1) and simplify to get

$$0 < |F_k \varphi - F_{k+1}| < \frac{1}{F_{k+1}}$$

By a similar argument as the proof for Theorem 4.8, this proves that F_{k+1} approximates an integer multiple of φ and therefore lies close to the axis. □

Appendix B

Appendix to Table 4.1

We mention here that for the golden ratio slope system described in Section 4.1, one of the first analyses conducted was done by using an unconventional average computation which was wrong, but interestingly, produced better results. Consider Table B.1 to verify that the percentage of Fibonacci numbers brought about by multiples of the golden ratio is remarkably high at 96.14%. The original code did not account for the simultaneous merging of 3 threads. The average of threads a, b, c with slopes s_a, s_b and s_c respectively was computed as $\frac{\frac{s_a+s_b}{2}+s_c}{2}$. This resulted in the individual threads being weighted differently, and the outstanding results provide an indication that weighted averages might be favourable (as was proven correct, cf. Table 4.2). Still, they also show that this slope system cannot be the "right" one since an erroneous definition led to the best result.

Initial slopes	$\{k\varphi\}$	$\{k\sqrt{2}\}$	$\{k\frac{\sqrt{13}-1}{2}\}$	$k\{\sqrt{5}\}$
Fibonacci numbers [%]	96.14%	48.94%	30.69%	50.61%

Table B.1: The percentage of Fibonacci numbers observed in the thicknesses of final threads (using a botched average computation), for $n = 1$ to 100 starting threads and various initial slopes.

Appendix C

Appendix to Section 4.3.3

Here we present another toy model which might be of interest for the study of the cellular automaton. In this version, the initial slopes are chosen by the mapping $0 \to 3, 1 \to 1$ of the infinite Fibonacci word and generate the sequence $\frac{L_n}{F_n}$ of slopes. We note that the slopes converge to $\varphi + \frac{1}{\varphi} = \sqrt{5}$. This can be shown by comparing $\frac{L_n}{F_n}^2$ to 5. The resulting differences are[1]

$$-\frac{4}{1}, \frac{4}{1}, -\frac{4}{4}, \frac{4}{9}, -\frac{4}{25}, \frac{4}{64}, \cdots$$

Observe that they grow smaller for larger n and alternately are greater than and lower than 5. So we can apply the same proof as in Section 4.3.3, using the parameter $\theta = \sqrt{5}$.

[1]We thank Dr. Matthew Cook for pointing these out to us.

Bibliography

[1] A. Peter. Code for the two toy models. https://github.com/anna-peter/bachelor-thesis, 2022. [Online; accessed 18-September-2022].

[2] M. H. Albert, R. J. Nowalski, and D. Wolfe. *Lessons in Play*. A. K. Peters, Ltd., 2007.

[3] S. Beatty, N. Altshiller-Court, O. Dunkel, A. Pelletier, F. Irwin, J. L. Riley, P. Fitch, and D. M. Yost. Problems for solutions: 3173-3180. *The American Mathematical Monthly*, 33(3):159–159, 1926.

[4] Charles L. Bouton. Nim, a game with a complete mathematical theory. *Annals of Mathematics*, 3(1/4):35–39, 1901.

[5] M. Cook, U. Larsson, and T. Neary. A cellular automaton for blocking queen games. *Natural Computing*, 16:397–410, 2016.

[6] H. S. M. Coxeter. The Golden Section, Phyllotaxis, and Wythoff's Game. 1953.

[7] E. W. Weisstein. Mathworld — A Wolfram Web Ressource. https://mathworld.wolfram.com/GoldenRatio.html, 2022. [Online; accessed 6-September-2022].

[8] E. W. Weisstein. Mathworld — A Wolfram Web Ressource. https://mathworld.wolfram.com/BeattySequence.html, 2022. [Online; accessed 12-September-2022].

[9] G. G. Krishnan. Continued fractions — Notes for a short course at the Ithaca High School Senior Math Seminar. https://pi.math.cornell.edu/~gautam/ContinuedFractions.pdf, 2016. [Online; accessed 4-September-2022].

[10] A. Ilachinski. *Cellular Automata: a Discrete Universe*. World Scientific Publishing Company, 2001.

[11] U. Larsson. Blocking Wythoff Nim. 2010.

[12] B. Lynn. Continued fractions. https://crypto.stanford.edu/pbc/notes/contfrac/definition.html. [Online; accessed 2-September-2022].

[13] Mathcamp. Crash course on combinatorial game theory. https://www.mathcamp.org/files/yearly/2019/quiz/cgt.pdf, 2019. [Online; accessed 30-August-2022].

[14] K. B. Stolarsky. Beatty sequences, continued fractions, and certain shift operators. *Canadian Mathematical Bulletin*, 19(4):473–482, 1976.

[15] The On-Line Encyclopedia of Integer Sequences. Fibonacci numbers. https://oeis.org/A000045. [Online; accessed 6-September-2022].

[16] The On-Line Encyclopedia of Integer Sequences. Lower Wythoff sequence. https://oeis.org/A000201. [Online; accessed 5-September-2022].

[17] The On-Line Encyclopedia of Integer Sequences. Lucas numbers. http://oeis.org/A000032. [Online; accessed 6-September-2022].

[18] J. von Neumann. Theory of Self-reproducing Automata. *Edited by Arthur W. Burks*, 1966.

[19] Wikipedia contributors. Continued fraction — Wikipedia, the free encyclopedia. https://en.wikipedia.org/w/index.php?title=Continued_fraction&oldid=1106872654, 2022. [Online; accessed 2-September-2022].

[20] W. A. Wythoff. A modification of the game of Nim. *Nieuw Arch. Wisk*, 7(2):199–202, 1907.

Eidgenössische Technische Hochschule Zürich
Swiss Federal Institute of Technology Zurich

Declaration of originality

The signed declaration of originality is a component of every semester paper, Bachelor's thesis, Master's thesis and any other degree paper undertaken during the course of studies, including the respective electronic versions.

Lecturers may also require a declaration of originality for other written papers compiled for their courses.

I hereby confirm that I am the sole author of the written work here enclosed and that I have compiled it in my own words. Parts excepted are corrections of form and content by the supervisor.

Title of work (in block letters):

Merging Properties of a Cellular Automaton for Blocking Queen Games

Authored by (in block letters):

For papers written by groups the names of all authors are required.

Name(s):	**First name(s):**
Peter	Anna Mei
.	

With my signature I confirm that

- I have committed none of the forms of plagiarism described in the 'Citation etiquette' information sheet.
- I have documented all methods, data and processes truthfully.
- I have not manipulated any data.
- I have mentioned all persons who were significant facilitators of the work.

I am aware that the work may be screened electronically for plagiarism.

Place, date	**Signature(s)**
Zurich, 22.9.2022	

For papers written by groups the names of all authors are required. Their signatures collectively guarantee the entire content of the written paper.